Lawrence Berkeley Laboratory
UNIVERSITY OF CALIFORNIA

Submitted for publication

ORBITAL RECOUPLING DOMINANCE IN THE A = 20 ISOVECTOR GIANT M1 TRANSITION

C.J. Martoff, J.A. Bistirlich, K.M. Crowe, M. Koike, J.P. Miller, S.S. Rosenblum, W.A. Zajc, H.W. Baer, A.H. Wapstra, G. Strassner, and P. Truöl

December 1980

DIVISION

Prepared for the U.S. Department of Energy under Contract W-7405-ENG-48

DISCLAIMER

LBL-11914

Orbital Recoupling Dominance in the A = 20 Isovector Giant M1 Transition†

C.J. Martoff*, J.A. Bistirlich, K.M. Crowe, M. Koike**,
J.P. Miller***, S.S. Rosenblum, and W.A. Zajc

Lawrence Berkeley Laboratory
University of California
Berkeley, California 94720

H.W. Baer and A.H. Wapstra****

Los Alamos Scientific Laboratory
Los Alamos, New Mexico 87545

G. Strassner***** and P. Truöl

Physik-Institut der Universität Zürich
8001 Zürich, Switzerland

†This work was supported by the Division of Nuclear Physics of the U.S. Department of Energy under Contract W-7405-ENG-48.

* Present address: Physik-Institut der Universität Zürich
8001 Zürich, Switzerland

** Permanent address: Institute of Nuclear Science
Tokyo, Japan

*** Present address: Physics Department, Boston University
Boston, MA 02215

**** Permanent address: Instituut voor Kernphysisch Onderzoek
Amsterdam, The Netherlands

***** Present address: Laboratory for High-Energy Physics, ETH, c/o SIN
5234 Villigen, Switzerland

Abstract

The relative importance of orbital and spin flip terms in the M1 transition between the ground and 11.24 MeV states in ^{20}Ne is determined from a measurement of the analog transition ^{20}Ne(π^-,γ)^{20}F (1^+, 1.06 MeV) with stopped pions. The M1 amplitude contains only (47 $\pm$ 16)% spin flip, in agreement with published results of shell model calculations. Excitation of 2^--states by ^{20}Ne(π^-,γ) is also observed.

In the systematic study of isovector M1 transitions (1) in the 1p- and 2s/1d-shell, the simultaneous analysis of radiative width measurements, inelastic electron scattering form factors and Gamow-Teller decays from the isobaric analog levels in neighboring nuclei (2) has allowed one to separate the two contributions to the M1 transition density due to the orbital current and spin magnetization, and thus to sharpen the comparison with nuclear model calculations. In general, spin flip dominates the transition density, since it is enhanced over the orbital part by the magnetic moment factor $\mu_p - \mu_n = 4.7$. For certain 1p-shell nuclei (^{6}Li (3,4), ^{12}C (5)) the radiative pion capture reaction has been measured with sufficient accuracy to obtain Gamow-Teller matrix elements. Furthermore, it was recently demonstrated that for M3 transitions in the 1p-shell, where only spin flip matrix elements are allowed, that the (e,e') and (π^-,γ) data give identical results (6).

We have measured the photon spectrum for the ^{20}Ne$(\pi^-,\gamma)^{20}$F-reaction with the goal of using branching ratios to directly extract spin density matrix elements. We chose ^{20}Ne since backward inelastic electron scattering (7) shows a strong isovector M1 transition to the 1^+-state at 11.24 MeV. Its analog occurs at 1.06 MeV in ^{20}F. Recent shell model calculations (8) show that $0^+ \rightarrow 1^+$ transitions in the sd-shell are different from those previously studied with (π^-,γ) in the 1p-shell, in that orbital recoupling tends to contribute as much to the amplitude as does spin flip. Our present study shows that the radiative pion capture reaction provides an excellent means for testing this kind of prediction.

The experimental apparatus consisted of a cryogenic liquid neon target 1.6 cm thick and 8.9 cm in diameter, and an electron-positron pair spectrometer similar to that described previously (9). The present improved system used multiwire proportional chambers instead of spark chambers, thinner converter foils, and new analysis codes. The trajectory coordinates measured by the MWPCs were converted analytically into the photon vector momentum, following an algorithm described in detail elsewhere (10). The lineshape and efficiency of the instrument and analysis system were calibrated on data taken with the neon target cell filled with liquid hydrogen. The resolution for the monochromatic 129.4 MeV photons from $\pi^- p \rightarrow n\gamma$ is 850 keV FWHM.

The photon spectrum for Ne is shown in Fig. 1. The contribution from the target container has been subtracted, but there is no correction for the 9.2% ^{22}Ne present in the natural Ne target. Since the photon energy for ^{22}Ne(π^-,γ)^{22}F (g.s.) is lower by 3.83 MeV than for ^{20}Ne(π^-,γ)^{20}F (g.s.), our discussion below is not affected by this. Transitions are seen leading to a group of states at low excitation in ^{20}F, and another group at about 6 MeV excitation. In addition, there is the photon continuum due to break-up capture.

The group of states at low excitation, identified with arrows in the inset of Fig. 1, are the 2^+-ground state, a 1^+-level at 1.06 MeV excitation, and two 2^--levels at 1.31 and 1.84 MeV. The three latter states are not resolved, but their relative contributions can be determined from a fit to the spectrum since the line shape and the energy scale are well known from hydrogen data and runs on other targets (^{12}C, ^{13}C, ^{19}F) measured in the same experiment (11). The results of the fit are given in Table 1. We repeated the fit, keeping the relative positions of the levels fixed, but varying the positions of the first one by ±200 KeV, twice the expected error on our abolute energy scale. A minimum in the overall chi-squared was found at the position expected kinematically. The error given for the branching ratios includes the uncertainty in the stopped pion flux and detector acceptance. We also include in Table 1 a branching ratio for the 6 MeV levels and the total spectrum. The 6 MeV structure most probably corresponds to a 2^--state similar to those previously observed (12) in ^{16}O and ^{12}C, and as predicted with about twice the observed branching ratio in the core-interaction separable interaction model (CESIM) (13,14). The combined strength of the 1.31 and 1.84 MeV 2^--states is approximately predicted by this theory, too.

The measured branching ratio for the 1^+-level is surprisingly small when compared to other transitions in the 2s/1d-shell (3,20). This can be understood with the phenomenological analysis presented below, and also on the basis of the Wildenthal-Chung wave functions for ^{20}Ne (8).

Over 90% of the pions are captured from the 2P atomic orbital in Ne (15). For a 0^+ to 1^+ transition we have the following expression for the transition rate (6,16-18) in the impulse approximation:

$$W_{fi} = \frac{16\pi^2 k_\gamma}{m_\pi(2J_i+1)(2\ell_\pi+1)} \frac{1+\frac{m_\pi}{m_A}}{1+\frac{k_\gamma}{m_A}} \left\{ \sum_{J,L} |\langle J_f \| \sum_{n=1}^{A} M_a(J,L,\ell_\pi;r_n) \| J_i \rangle|^2 \right. \qquad |1|$$

$$\left. + |\langle J_f \| \sum_{n=1}^{A} M_b(J,L,\ell_\pi;r_n) \| J_i \rangle|^2 \right\}$$

with

$$M_a(1,2,1) = \frac{K_{2p}}{\sqrt{4\pi}} \left[\left\{ Arj_1 + k(B+C)j_0 \right\} t_+ [\sigma x Y_0]^1 - 3\sqrt{2} \left\{ \frac{rA}{5}(j_3 + \frac{j_1}{6}) \right. \right. \qquad |2|$$

$$\left. \left. + \frac{k}{3}(\frac{B}{2} - C)j_2 \right\} t_+ [\sigma x Y_2]^1 \right]$$

$$M_b(1,1,1) = \frac{K_{2p}}{\sqrt{4\pi}} \left[\left\{ -Arj_1 + 1(C-B)j_0 \right\} t_+ [\sigma x Y_0]^1 \right. \qquad |3|$$

$$\left. + \frac{1}{\sqrt{2}} \left\{ -Arj_1 + k(B+2C)j_2 \right\} t_+ [\sigma x Y_2]^1 \right]$$

$K_{2p} = \frac{1}{2\sqrt{6}} \sqrt{C_{2p}}\, a_\pi^{-5/2}$ C_{2p} = pionic wave function distortion factor (19) = 1.18, value for ^{16}O, ref. 20.

a_π = Bohr radius of pionic atom, and A, B, C = coefficients of the (π^-,γ)-Hamiltonian (11,16)

and with the notation of Ref. 16.

The measured quantity is the radiative capture branching ratio which is the radiative capture rate divided by the total width of 2p pionic neon (21). We have considered the effect of a 5-10% 1S-state capture and found this not to affect our conclusions.

Evaluating the radial matrix elements in Eq. |1| using harmonic oscillator wave functions with r_o = 1.835 fm (22), the measured branching ratio gives a constraint on the sum of squares of the reduced matrix elements

$$R_{01} = \langle 1^+ \| t_+ [\sigma x Y_0]^1 \| 0^+ \rangle \quad \text{and} \quad R_{21} = \langle 1^+ \| t_+ [\sigma x Y_2]^1 \| 0^+ \rangle \quad . \qquad |4|$$

We obtain

$$1 = \frac{|R_{01}|^2}{(.12)^2} \quad \frac{|R_{21}|^2}{(.46)^2} \quad \frac{\mathrm{Re}\,|R_{01} R_{21}^*|}{(1.04)^2} \quad . \qquad |5|$$

The M1 width for electromagnetic decay of the 11.24 MeV state in ^{20}Ne to the ^{20}Ne ground state is given by (2)

$$\Gamma_{\gamma,0}(1^+ \rightarrow 0^+) = \frac{2\pi\alpha}{9} E_\gamma^3 \frac{1}{m^2} \left| \frac{g_p - g_n}{2} R_{01} + L_{01} \right|^2 \qquad |6|$$

with

$$\tfrac{1}{2}(g_p - g_n) = 4.7 \text{ and } L_{01} = \langle 1^+ \| t_+ [L x Y_0]^1 \| 0^+ \rangle \; .$$

R_{01} denotes the matrix element of the spin current and L_{01} denotes the matrix element of the orbital current. Eq. |5| indicates that the (π^-,γ) branching ratio is rather insensitive to R_{21}. Neglecting R_{21} altogether, we use Eq. |5| to obtain $R_{01} = 0.12 \pm 0.04$. We use Eq. |6| together with the experimental value for $\Gamma_{0,\gamma}$ of (11.2 ± 2.0) eV (7) to obtain $4.7\ R_{01} + L_{01} = 1.17 \pm 0.1$. Combining these two values, we obtain $L_{01} = 0.62 \pm 0.21$. The orbital term is thus seen to account for 53 ± 16% of the amplitude of Eq. |6|.

Full sd-shell model calculations (8) predict the values $R_{01} = 0.105$ and $L_{01} = 0.605$ leading to $\Gamma_{0,\gamma} = 10$ eV and a (π^-,γ) branching ratio of $(0.74 \pm 0.14) \times 10^{-4}$, in agreement with our measured value of (0.9 ± 0.5) 10^{-4}. The small R_{01} value can be traced to the sign difference between the dominant $5/2 \rightarrow 5/2$ and $3/2 \rightarrow 5/2$ spin density matrix elements (8).

The situation here is quite different from that in the 1p-shell. In the A = 12 system, for example, spin flip accounts for 95% of the M1 amplitude (5). The excitation of giant M1 levels by radiative pion capture has been observed to closely follow the pattern of inelastic electron scattering strength throughout the 1p-shell nuclei (3,6,20,23). This is the first case to be analyzed in detail in which nuclear structure effects alter significantly the close analogy between the spin flip processes dominating (π^-,γ) and the electromagnetic M1 operator.

In summary, the $^{20}Ne(\pi^-,\gamma)^{20}F$-reaction has been used in combination with inelastic electron scattering to separate the M1 operator into its spin flip and orbital current parts. The giant M1 transition in A = 20 is shown to have an important contribution from the orbital term, in agreement with theory. The utility of the (π^-,γ)-reaction for directly measuring the spin flip matrix elements has been demonstrated.

References

1 L.W. Fagg, Rev. Mod. Phys. 47, 683 (1975).

2 S.S. Hanna, in "Isospin in Nuclear Physics", D.H. Wilkinson, ed., North-Holland, Amsterdam (1969) p. 591.

3 J.P. Perroud, in "Photopion Nuclear Physics", P. Stoler, ed., Plenum Press, New York (1979) p. 69.

4 J.C. Bergstrom, Phys. Rev. C21, 2496 (1980).

5 W. Maguire, C. Werntz, Nucl. Phys. A205, 211 (1973).

6 A. Perrenoud et al., to be published; cited in P. Truöl in "Nuclear Physics with Electromagnetic Interactions", Lect. Notes in Physics 108, Springer, Berlin (1979) p. 351.

7 W.L. Bendel et al., Phys. Rev. C3, 1821 (1971).

8 B.H. Wildenthal, W. Chung, Michigan State University, Preprint (1979), and Contribution 1.8 to Int. Conf. on Nucl. Phys. with Electromagnetic Intns., Mainz, Germany (June 1979).

9 J.A. Bistirlich et al., Phys. Rev. C5, 1867 (1972), and references given in Ref. 11.

10 J.C. Alder et al., Nucl. Instr. and Meth. 160, 93 (1979).

11 C.J. Martoff et al., to be published.

12 G. Strassner et al., Phys. Rev. C20, 248 (1979).

13 W. Knüpfer, H. Ender, M.G. Huber, private communication; see also contributed paper to VIII Int. Conf. on High-Energy Physics, Vancouver (1979).

14 W. Knüpfer et al., Phys. Lett. 66B, 305 (1977).

15 W.W. Sapp et al., Phys. Rev. C5, 690 (1972). Values are given for ^{19}F and ^{23}Na; the 2P capture fraction scales smoothly with Z.

16 H. Ohtsubo et al., Nucl. Phys. A224, 164 (1974).

17 N. Ohtsuka, thesis, Osaka University, Japan (1974).

18 A. Perrenoud, thesis, Université de Lausanne, Switzerland (1979).

19 V.V. Balashov, G.J. Korenman, R.A. Eramzhyan, "Capture of Mesons by Atomic Nuclei", Atomizdat, Moscow (1978).

20 For a review see H.W. Baer, K.M. Crowe, P. Truöl, Adv. Nucl. Phys. 9, 177 (1977).

21 We interpolate the ^{19}F and ^{22}Na-values given by G. Backenstoss, Ann. Rev. Nucl. Sci. 20, 467 (1970) to obtain $\Gamma_{2P}(^{20}\mathrm{Ne}) = (20 \pm 7)$ eV.

22 J. Zofka, G. Ripka, Nucl. Phys. A168, 65 (1971).

23 H.W. Baer, Proc. VII Int. Conf. on High-Energy Phys. and Nucl. Structure, M. Locher, ed., Birkhäuser, Basel (1977) p. 245.

Table 1. $^{20}Ne(\pi^-,\gamma)^{20}F$ Partial Branching Ratios*

E_γ	$E_x[^{20}Ne]$	J^π	$E_x[^{20}F]$	N^a	$R_\gamma[10^{-4}]^c$	$R_\gamma/R_\gamma^{tot}[10^{-2}]^b$
131.31	10.27	2^+	0.0	71 ± 13	0.7 ± 0.3	0.42 ± 0.08
130.25	11.24	1^+	1.06	97 ± 58	0.9 ± 0.5	0.57 ± 0.34
130.01	11.57	2^-	1.30	182 ± 70	1.7 ± 0.6	1.07 ± 0.41
129.47	12.11	2^-	1.84	274 ± 32	2.6 ± 0.3	1.61 ± 0.19
125.2[d]	16.4	$[2^-]$	6.1	1630 ± 80	15.3 ± 2.	9.55 ± 0.47
114.2[e]	27.4		17.1	511 ± 160	4.8 ± 1.7	3.0 ± 0.9
pole[f]				14300 ± 370	134. ± 20.	84. ± 2.2
Total				17,065	160 ± 24	100.

*All energies are given in MeV.

a) Number of events in spectrum obtained in the fit, corrected for the energy dependence of the efficiency curve. Uncertainties are from fitting only.

b) Relative branching ratios, uncertainties from fitting only.

c) Absolute branching ratios including uncertainty in normalization.

d) Breit-Wigner-Shape, full width 1.35 MeV.

e) as d, full width 2.7 MeV.

f) Spectrum for quasifree radiative capture (20) leading to ^{19}F ground state $^{20}Ne(\pi^-,\gamma n)^{19}F$, pole model Δ = 14.14 MeV.

Figure caption

Figure 1

Inclusive photon spectrum from $^{20}Ne(\pi^-,\gamma)$, with photon energy scale in MeV and vertical scale in events per 0.2 MeV. The excitation energy scale in ^{20}F is also shown. Inset: enlarged view of upper part of photon spectrum shown in Fig. 1, and the fit to 4 lines folded with the instrumental line shape. Spin parity assignments are from Ajzenberg-Selove, Nucl. Phys. A300, 1 (1978), Table 20.4.

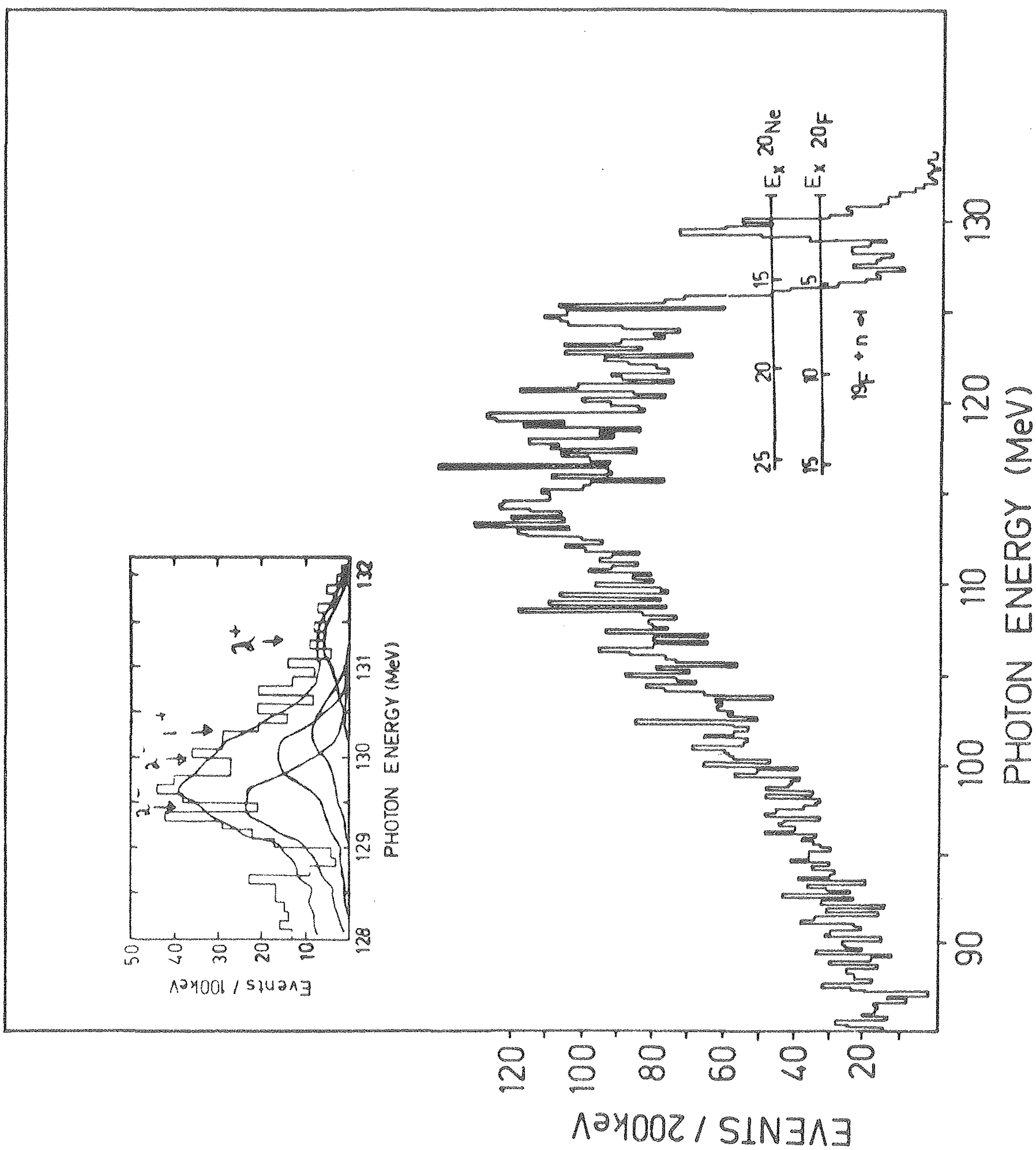
EVENTS / 200keV
PHOTON ENERGY (MeV)
Events / 100keV
PHOTON ENERGY (MeV)
Ex 20Ne
Ex 20F
19F + n

Fig. 1.